Generation of Two-Dimensional Correlated Shadowing for Mobile Radio Network Simulation

Ingo Forkel, Marc Schinnenburg, Markus Ang
Communication Networks, Aachen University, Germany
Email: ingo.forkel@ieee.org

***Abstract*— An integral aspect of radio propagation especially outside of buildings is the loss due to shadow fading (also known as long-term fading). This is caused by the presence of obstacles which lie in the propagation path of the radio waves. While modeling the shadow fading loss, the spatial, angular and temporal correlation of the shadow fading values has to be considered. By that, it is taken into account that an obstacle which lied in the propagation path during the last measurement of the radio wave cannot simply disappear at the following measurement. Moreover, signals coming from the same direction experience a similar shadow effect and the location dependency of the shadow fading values makes sure that another mobile at the same location also gets the same signal attenuation.**

This article aims at generating shadow fading profiles which can be used in simulations of realistic mobile radio network scenarios. The focus is on achieving two-dimensional spatial correlation of the shadow fading values. Methods for introducing the angular and temporal correlation are explained in addition. Simulations with the different shadow fading profiles are run and comparisons between quality-of-service (QoS) aspects obtained with these profiles are presented.

I. Introduction

For emulating and simulating realistic mobile radio networks, the propagation of electro-magnetic waves inevitably has to be carefully modeled. An integral aspect of radio propagation besides path loss and multi-path fading is the loss due to shadow fading, also known as shadowing or long-term fading. This is caused by the presence of obstacles which lie in the propagation path of the radio waves, e.g. houses, trees, furniture, etc. [1], [2]. Hence, shadow fading represents signal fluctuations around the average path loss due to man-made (buildings, cars, walls, etc.) or natural (hills, rain, trees, etc.) obstructions in the way of a propagating electro-magnetic wave. Thus, waves are prevented from traveling the most direct and shortest path (usually also the path with least attenuation) between a transmitter and a receiver.

The shadow fading value L_s is usually characterized by a Gaussian (normal) distribution in the logarithmic scale with zero mean and certain standard deviation in the magnitude of 8–10 dB dependent on the environment as recommended in [1], [3]. The probability density function (PDF) is given by

$$p(L_s) = \frac{1}{\sigma_{L_s}\sqrt{2\pi}} e^{-\frac{(L_s-\mu_{L_s})^2}{2\sigma_{L_s}^2}}, \qquad (1)$$

with standard deviation σ_{L_s} and mean μ_{L_s}. In linear scale, shadow fading follows a log-normal distribution. For this reason it is also called log-normal fading.

It is obvious that the shadow fading values depend on the terrain and the surrounding property in the vicinity of the mobile. These values have to show a spatial correlation due to the fact that terrain and morphology structure do not change abruptly. Moreover, another user should experience similar shadow fading effects when passing by the same location. Hence, one of the most difficult aspects of shadow fading is to find an accurate correlation model. Several methods have been used to generate random shadow fading variables in order to achieve certain autocorrelation and have been used in past simulations.

Based on measurements conducted in urban areas, a link-based autocorrelation model is proposed in [4]. This model is supposed to be adopted when simulating 3rd generation mobile cellular networks based on wideband code division multiple access (WCDMA) as in [3]. But the model treats all links independently on each other, i.e. the correlation is only based on the user's movements through the scenario on a time basis. If multiple links have to be considered in parallel as in the so-called soft handover state of a user equipment (UE) or also while measuring the neighbouring cells' pilot signals, this model can not provide certain correlation properties between the different links.

In [5], the model is extended in order to also capture cross-correlation of shadow fading variables for links to multiple base stations. Thus, a single user experience realistic shadow fading effects to the surrounding base stations and not only to the serving station. A similar approach has been already given by [6] where the angular correlation is modeled with an exponentially decaying function dependent on the angle between the links under consideration.

Whereas these models are focussed on shadow fading calculation on a per-link basis, [7] proposes a two-dimensional model where the shadow fading values are location-based. This kind of shadow fading map also captures the effect that identical or at least similar values are seen by mobiles at the same position within the scenario.

In this paper, we describe a shadow fading model which combines the advantages of the different models presented before, i.e. local and time correlation of the shadow fading values, cross-correlation (or angular correlation) between multiple links and dependency on the absolute position of a mobile in the simulation scenario. Moreover, the generation of random variables that adhere to such a location-based correlation is the main objective of this contribution.

The remainder of this paper is organized as follows. The different correlation properties under study are highlighted in Sec. II. We also focus on the application of the generated variables for mobile network simulations with respect to temporal and local interpolation. In Sec. IV, performance differences in a simulated universal mobile telecommunications system (UMTS) network example are evaluated taking into account differently generated shadow fading maps. By means of such dynamic system-level simulations the effects of outage durations as a result of shadow fades are addressed not only in an analytical manner as in [8] but also with reference to the location within the simulated scenario. Certain network and link-based quality-of-service (QoS) criteria can be evaluated.

II. Correlation Model for Shadow Fading

When generating random variables for the shadow fading the first criteria is that the variables in the logarithmic scale must follow a Gaussian distribution as in (1). The variables should be distributed in such a way that their mean μ_{L_s} is 0 and the standard deviation σ_{L_s} is 10 dB [3] in case of urban scenarios for UMTS networks.

The two-dimensional shadow fading values are subject to three different kinds of correlation processes. Spatial correlation considers the fixed location of obstacles, angular correlation reflects the direction to or from the base station(s) relevant for a user in the scenario, and temporal correlation prevents from sudden changes in

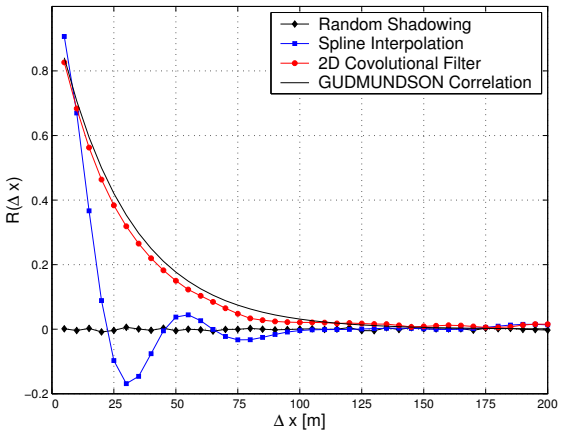

Fig. 1. Autocorrelation functions plots of random (uncorrelated), spline interpolated, and convoluted shadow fading variables

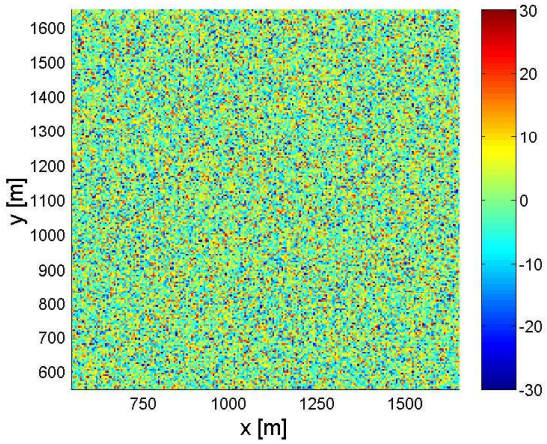

Fig. 2. Example two-dimensional shadow fading map with random (uncorrelated) shadow fading variables

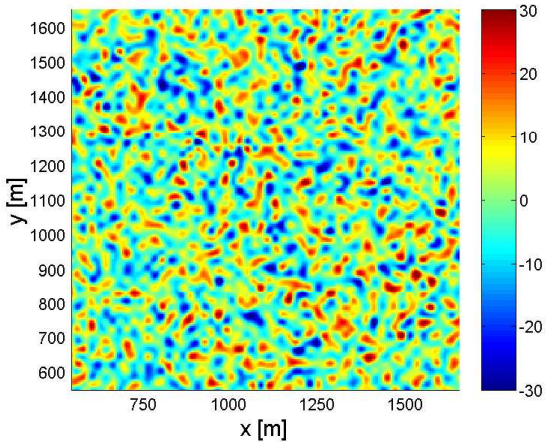

Fig. 3. Example two-dimensional shadow fading map with spline interpolated shadow fading variables

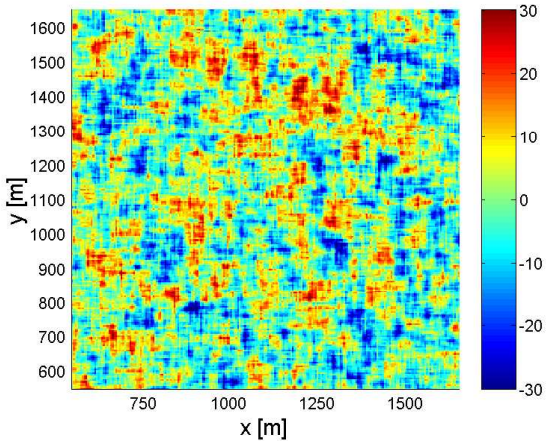

Fig. 4. Example two-dimensional shadow fading map with convolutional correlated shadow fading variables

the shadow fading value by traveling across the tiles of the shadow fading map which obviously has a restricted resolution Δs. In the following, a shadow fading map with dimensions $2.5 \times 2.5\,\mathrm{km}$ and a resolution of $2.5\,\mathrm{m}$ is taken into account.

A. Spatial Correlation

In [4], a one-dimensional model for the spatial correlation properties is given for suburban and urban environments. The normalized autocorrelation function $R(\Delta x)$, where Δx is the change in distance, can be described with sufficient accuracy by an exponential function as

$$R(\Delta x) = e^{-\frac{|\Delta x|}{d_{\mathrm{corr}}} \ln 2}, \tag{2}$$

with the decorrelation length d_{corr}, which is dependent on the environment. For the urban vehicular test environment (VTE), [3] proposes $d_{\mathrm{corr}} = 20\,\mathrm{m}$. This correlation works satisfactorily for distances up to approximately $500\,\mathrm{m}$. Although the second derivative at the origin of this autocorrelation function is not defined (as requested by [8]), it does not lead to sharp changes of shadow fading values when embedded into a two-dimensional map with finite resolution. Moreover, an interpolation process as described in Sec. II-C prevents from such effects.

In the following, three different methods of generating two-dimensional shadow fading variables are discussed. The resulting autocorrelation functions and a cut-out of the generated shadow fading map are given in Fig. 1 and Fig. 2 to Fig. 4, respectively.

1) Random Variables: For a simulation scenario with locally dependent obstruction effects, we will need to somehow obtain a matrix of shadow fading variables $L_s(x, y)$ that depends on the size of the scenario and a given resolution as illustrated in Fig. 2. However, it is not possible to generate truly random numbers with the help of computer processors. They can be supplied by external sources like radioactive decay. Such sequences are available (e.g. on magnetic tape), but clumsy to use and often not sufficient in terms of speed and number [9]. For most purposes, it is sufficient and much easier to rely on pseudo-random number generators. Pseudo-random numbers are a sequence of numbers generated by an algorithm in a way that the resulting numbers look statistically independent and uniformly distributed. This is the prevailing method used for computer simulations.

By examining the autocorrelation function properties of the variables, we see that the variables show no correlation at all (see Fig. 1). The correlation properties of (2) are not fulfilled for randomly generated shadow fading values.

2) Spline Interpolation: To improve the correlation properties of the variables, a spline interpolation method is used. What the spline interpolation does is basically to connect two adjacent points with a smooth curve considering as well the neighboring points related to the two that are joined. Therefore, the shadow fading map is created with lower resolution and then spline interpolated to $\tilde{L}_s(x, y)$ achieving the same resolution as before. Here we have chosen the resolution of the preliminary map to be equal to the

decorrelation length d_{corr}. The resulting interpolated shadow fading map (Fig. 3) looks less noisy compared to uncorrelated values.

Fig. 1 once again shows the autocorrelation of these spline interpolated variables. We can see that they indeed do show a better correlation. However, after the interpolation process the mean and the standard deviation of the variables had to be corrected by using

$$\tilde{L_s}'(x,y) = \left(\tilde{L}_s(x,y) - (\mu_{\tilde{L}_s} - \mu_{L_s})\right) \cdot \frac{\sigma_{L_s}}{\sigma_{\tilde{L}_s}} \qquad (3)$$

in order to stay in line with the requirements of [3].

3) Two-Dimensional Convolution: As observed in the previous sections, the generated variables do not meet the autocorrelation criteria. The two-dimensional convolution method of generating the shadow fading variable aims at fulfilling the desired criteria.

Since the shadow fading map is two-dimensional, we will need to employ the two-dimensional convolution. Consider two $(N_x \times N_y)$-matrices $\mathbf{L_s}$ and $\mathbf{C_s}$, where $\mathbf{L_s}$ are randomly generated shadow fading variables and $\mathbf{C_s}$ contains one row and column of autocorrelation coefficients determined with the help of (2), respectively. The resulting matrix $\tilde{\mathbf{L}}_\mathbf{s} = \mathbf{L_s} * \mathbf{C_s}$ after a two-dimensional convolution is given by its elements

$$\tilde{L}_s(x,y) = \sum_{i=1}^{N_x} \sum_{j=1}^{N_y} L_s(i,j) C_s(x-i+1, y-j+1). \qquad (4)$$

To achieve the autocorrelation between the variables, we first calculate a set of autocorrelation coefficients using (2) where Δx varies between 0 to the dimension of the scenario by the desired resolution. Gaussian distributed random variables are generated and convoluted two-dimensionally with the calculated autocorrelation coefficients.

Convolution does not alter the distribution of the variables as it acts like a finite impulse response (FIR) filter. Thus, the new variables still follow the Gaussian distribution. However, the mean and the standard deviation of the variables change and have to be corrected using (3).

This method of generating variables has shown an autocorrelation that almost matches (2). The corresponding curve in Fig. 1 confirms the correlation. From the shadow fading map in Fig. 4 it is visualized that there is a clear correlation between the variables.

B. Angular Correlation

If a shadow fading map is generated as described above, angular correlation can be considered with the help of neighbouring tiles. To achieve correlation for a certain range of directions, we can simply take the neighbouring shadow fading value laying in this direction instead of the one the mobile is actually on as illustrated in Fig. 5.

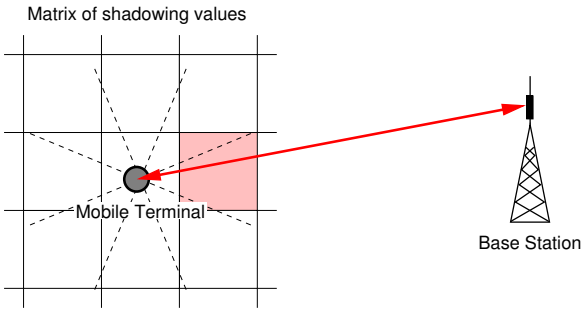

Fig. 5. How to achieve angular correlation of the shadow fading variables

The resulting angular autocorrelation function is defined stepwise with the resolution of $2\pi/9$ and the correlation properties are determined by the spatial correlation of the shadow fading variables.

C. Temporal Correlation

In order to achieve temporal correlation of the shadow fading values, the base values of the tiles have to be interpolated in a smooth way. With a precedent value $L_s(\tau_k)$ at a given time instant k, the subsequent value at time $k+1$ is recursively determined by

$$L_s(\tau_{k+1}) = L_s(\tau_k) + \frac{k \bmod n}{2n - (k \bmod n)}(L_{s,\text{new}} - L_s(\tau_k)), \quad (5)$$

where $L_{s,\text{new}}$ is the shadow fading value at a target location. After an update interval of n measurement cycles, the value has to be re-determined. The length of the update interval n is dependent on the duration of a measurement cycle t_{meas} which is equal to the frame duration of 10 ms or even slot duration of 667 ns in a WCDMA network, the velocity v of the user, and the resolution Δs of the shadow fading map. It is determined by

$$n = \frac{\Delta s}{v \cdot t_{\text{meas}}}. \qquad (6)$$

It is important to reset k if the velocity of the user or the measurement interval changes, i.e. when entering a different road category or perform an inter-system handover e.g. between GSM and UMTS.

III. Simulation Environment

The event-driven *Generic Object Oriented Simulation Environment* (GOOSE) is used for simulation purposes which has been extensively used for the simulation of UMTS networks including soft handover, fast power control and radio resource management issues [10]–[12]. Fig. 6 depicts the graphical user interface of the tool developed at ComNets. As a simulation scenario, a real network deployment in the urban area of Amsterdam is recreated considering 7 sites each equipped with three sectors. The figure shows the best server areas (by different colors) and we can clearly identify the 120 degree sectors of the Node B. Moreover, the patchwork of best server areas at the cell borders due to the location and direction based shadow fading variables is visible.

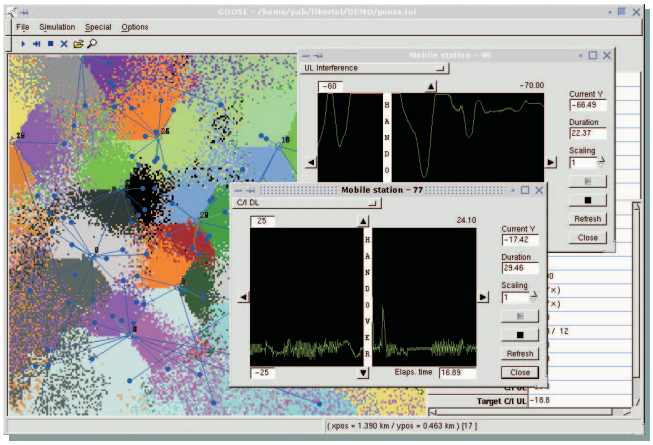

Fig. 6. GOOSE graphical user interface

Propagation characteristics, user's mobility along streets or railways with velocities between 3 and 50 km/h and certain turning properties at intersections, and antenna patterns follows the guidelines as given in [13]. Power control inaccuracies and channel estimation errors are combined in a Gaussian distributed random error with standard deviation of 1 dB.

Traffic is circuit switched speech service at 12.2 kbps with an activity of 50% [3]. Estimation of the user bit error ratio (BER) in order to determine for satisfied users follows the analytical studies in [14]. The results vary with respect to the differing shadow fading variables used for the radio propagation modeling.

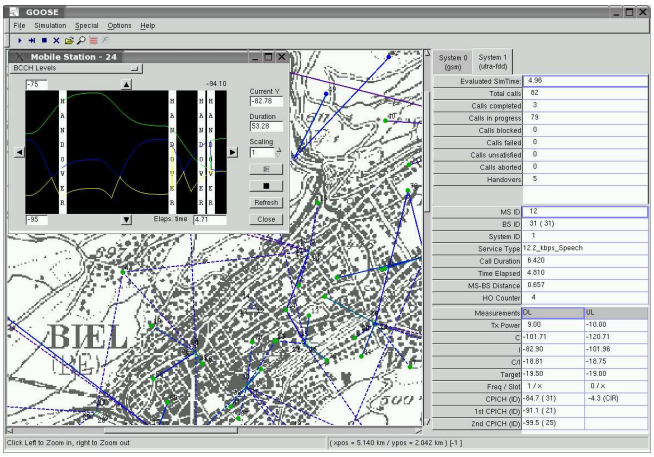

Fig. 7. Simulation scenario comprising GSM and UMTS with CPICH measurements of one particular mobile

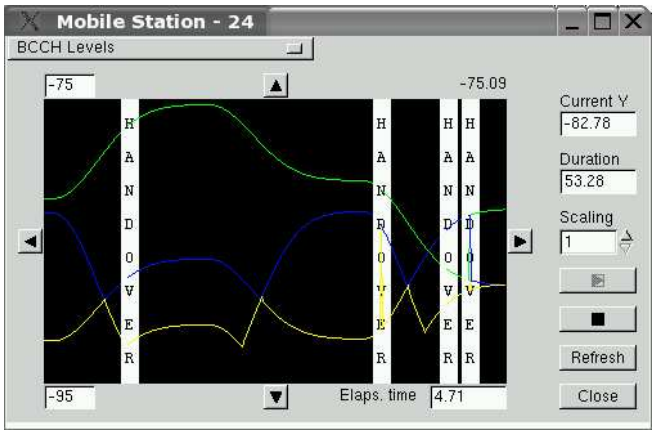

Fig. 8. Shadow fading process for the three strongest CPICH signals of different Node Bs in GOOSE

Fig. 7 illustrates the mobile users traveling through a realistic scenario of Biel, Switzerland. The window for the pilot measurements of a particular UE are included in this screen shot.

Fig. 8 illustrates the shadow fading process exemplarily for the three strongest common pilot channel (CPICH) measurements of this UE in the center of the scenario. Fast fading and channel estimation errors in this example are turned off. We can see that the serving base station experiences smooth shadow fading while the UE is traveling through the scenario. One CPICH signal which at the beginning shows the weakest reception level follows a similar shadow fading process. These two signals belong to different sectors of the same site and experience the same shadow fading due to the angular correlation of the direct links. Another CPICH signal can be seen which shows a different behavior because of opposite link directions. The graphical representation offers only the three strongest pilot signals and we can't go into the details for the weaker links but we can conclude that the above described model provides satisfactory results.

IV. Simulation Results

The interests of network operators is if they are able to provide a certain quality of service (QoS) to their customers. Thus, based on criteria set out in [3], the satisfaction of a user dependent on call admittance, connection quality (no failure and sufficient voice quality) and handover success (no call abort) is examined. Fig. 9 shows the fraction of satisfied users at different offered traffic. The three curves in the result plots correspond to the random shadow fading (Random), the spline interpolated values (Spline), and the convolutional correlated (Correlated) shadow fading variables, respectively.

It can be observed that there are only a very small number of users who are satisfied if shadow fading is a random process. This means that neighboring points of a map may have a sudden change in total path loss due to shadow fading. This eventual drastic change in the path loss may result in calls being aborted because the network is not able to adjust the transmission power or to perform a handover fast enough.

In the case of the correlated and spline interpolated values, we expect no sudden change in shadow fading values at adjacent points and thus it is realistic to expect that at low loads, the network should be able to satisfy almost all of its customers. At high loads however, there will always be a certain amount of unsatisfied users due to call blocking and high interference [13]. It is relatively clear that for simulation purposes where shadow fading is considered, a random shadow fading map is not very useful.

The above results can also be explained when looking at the cumulative distribution function (CDF) of the downlink carrier-to-interference ratio (CIR) as plotted in Fig. 10. A large fraction of the CIR measurements are substantially lower when using the random map as compared to the correlated or spline interpolated shadow fading. With respect to a minimum CIR of -20 dB where connection can still be considered satisfactory, we observe almost 40% of the measured values below this limit for the random values. In the case of the correlated and spline interpolated shadow fading values, it is only about 7%.

The plots in Fig. 11 and Fig. 12 show the transmission power per channelization or spreading code, i.e. connection, in uplink and downlink direction with respect to the distance to the serving Node B. For the downlink transmission power we did not consider the power necessary for the common control channel (CCCH) and the common pilot channel (CPICH).

There is an average of about 10–20 dB difference in the transmission power between the correlated and spline interpolated maps. With the random variables, no reasonable communication is possible because power control is simply adjusting to the upper limits. The higher transmission powers necessary at close distance to the Node B are due to the antenna characteristics which shows significant losses between the main lobe and the first side lobe. With increasing distance the average uplink transmission power tends towards the maximum level of 21 dBm and leaves almost no headroom to compensate for fast or long-term fading.

V. Conclusion

In conclusion, we have described the generation of two-dimensional correlated shadow fading variables and examined in closer detail their effects on network simulations. An appropriate model of a shadow fading map is of great importance to obtaining accurate results.

Without consideration of shadow fading correlation properties, network simulation results are useless. In the spline interpolated map, we observe the best overall system performance due to the better correlation at close distances which means a smaller change in the total path loss as a user moves from one location to an adjacent location where measurements are taken. However, it may be questionable if the results are indeed realistic if we were to calculate the path loss based on these interpolated variables. Usage of two-dimensional convoluted shadow fading values gives the most realistic fading characteristics, but network performance is significantly affected.

This can be looked into more closely as well as to portrait the same characteristics in different simulation scenarios. Future work can additionally examine the difference in system performance if a

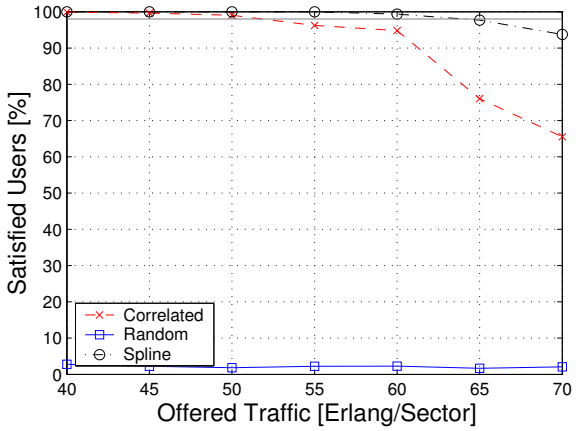

Fig. 9. Satisfied users according to [3] in the network dependent on the offered traffic, i.e. number of speech connections

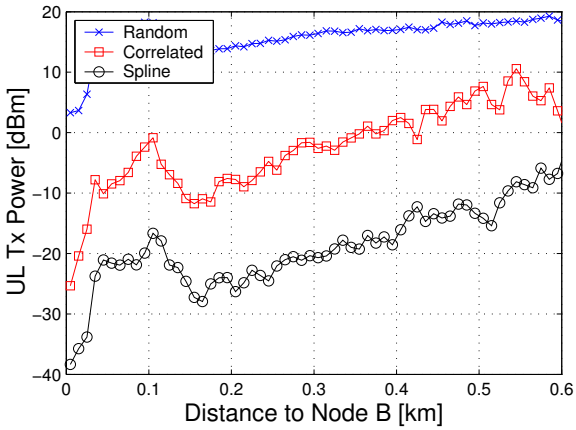

Fig. 11. Uplink dedicated channel Tx power at 60 Erlang/sector over distance to Node B

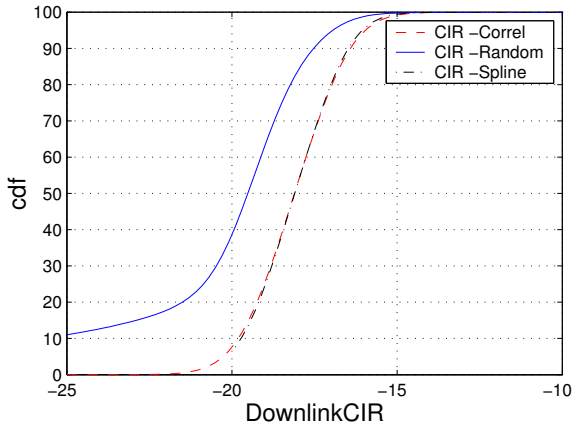

Fig. 10. Downlink CIR at 60 Erlang/sector

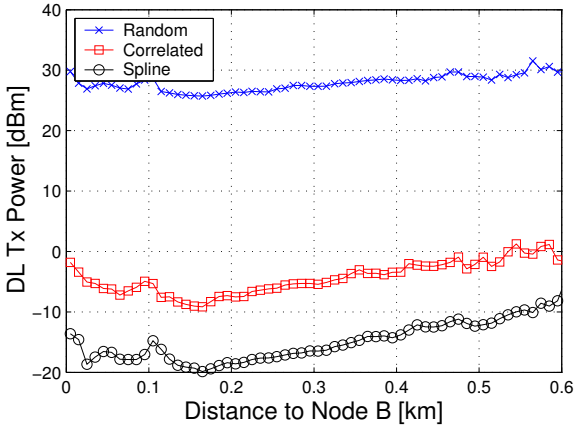

Fig. 12. Downlink dedicated channel Tx power at 60 Erlang/sector over distance to Node B

different decorrelation length or scenario resolution is assumed. Moreover, with respect to beamforming algorithms as a major topic for next generation networks, the inclusion of location-based correlated shadow fading is a key issue in propagation modeling for radio network simulations.

ACKNOWLEDGMENT

The authors would like to thank Prof. B. Walke of ComNets for his support and friendly advice to this work. The contributions of R. Pabst and the comments of the anonymous reviewers are highly appreciated. Development of the simulation tool, creation of the network scenarios and especially the validation with real field measurements would have never been possible without the support of Vodafone-Netherlands and Swisscom Mobile which the authors grateful acknowledge.

REFERENCES

[1] B. Walke, *Mobile Radio Networks*. Chichester, UK: John Wiley & Sons, 2001.
[2] W. Lee, *Mobile Communication Design Fundamentals*. New York: John Wiley & Sons, 1993.
[3] ETSI, "TR 101 112, Selection Procedures for the Choice of Radio Transmission Technologies of the UMTS (UMTS 30.03)," European Telecommunications Standards Institute, Tech. Rep., Apr. 1998.
[4] M. Gudmundson, "Correlation Model for Shadow Fading in Mobile Radio Systems," *Eltronics Letters*, vol. 27, no. 23, pp. 2145–2146, Nov. 1991.
[5] F. Graziosi and F. Santucci, "A General Correlation Model for Shadow Fading in Mobile Radio Systems," *Communication Letters*, vol. 6, no. 3, pp. 102–104, Mar. 2002.
[6] G. Malmgren, "On the Performance of Single Frequency Networks in Correlated Shadow Fading," in *Transactions on Broadcasting*, vol. 43, no. 3. IEEE, 1997.
[7] K. Kumaran, S. Golowich, and S. Borst, "Correlated Shadow-Fading in Wireless Networks and its Effect on Call Dropping," *Wireless Networks*, vol. 8, no. 1, pp. 61–70, Jan. 2002.
[8] N. Mandayam, P. Chen, and J. Holtzman, "Minimum Duration Outage for CDMA Cellular Systems: A Level Crossing Analysis," *Wireless Personal Communications*, vol. 7, no. 2/3, pp. 135–146, Aug. 1998.
[9] A. Law and W. Kelton, *Simulation, Modeling and Analysis*, 2nd ed. McGraw-Hill, 1991.
[10] I. Forkel, "Performance Comparison of Radio Access Technologies for the UMTS (Invited Paper)," in *Proc. Wireless Personal Multimedia Communications (WPMC)*, Yokosuka, Japan, Oct. 2003.
[11] M. Schinnenburg, I. Forkel, and B. Haverkamp, "Realization and Optimization of Soft and Softer Handover in UMTS Networks," in *Proc. European Personal and Mobile Communications Conference (EPMCC)*, Glasgow, Scotland, UK, Apr. 2003.
[12] I. Forkel and H. Klenner, "High Speed Downlink Packet Access (HSDPA) – A Means of Increasing Downlink Capacity in WCDMA Cellular Networks?" in *Proc. European Wireless*, Barcelona, Spain, Feb. 2004.
[13] I. Forkel, M. Schinnenburg, and B. Wouters, "Performance Evaluation of Soft Handover in a Realistic UMTS Network," in *Proc. VTC 2003 Spring*, Jeju, Korea, May 2003.
[14] S. Lin and D. Costello, *Error Control Coding*. Prentice-Hall, 1983.